

Input

BDN

ERRNet

IBCLN

Kim *et al.*

Chang *et al.*

Peng *et al.*

Ours



Synthesized input



Ground truth I_B



Ground truth I_R



(a)



(b)



(c)



(d)



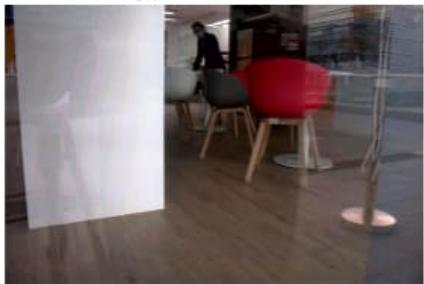
(a) M : Our ISP



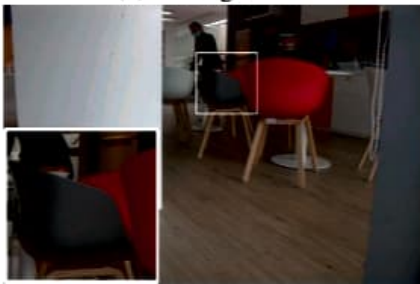
(b) M : Lightroom



(c) M : Camera



(d) M : Our ISP1

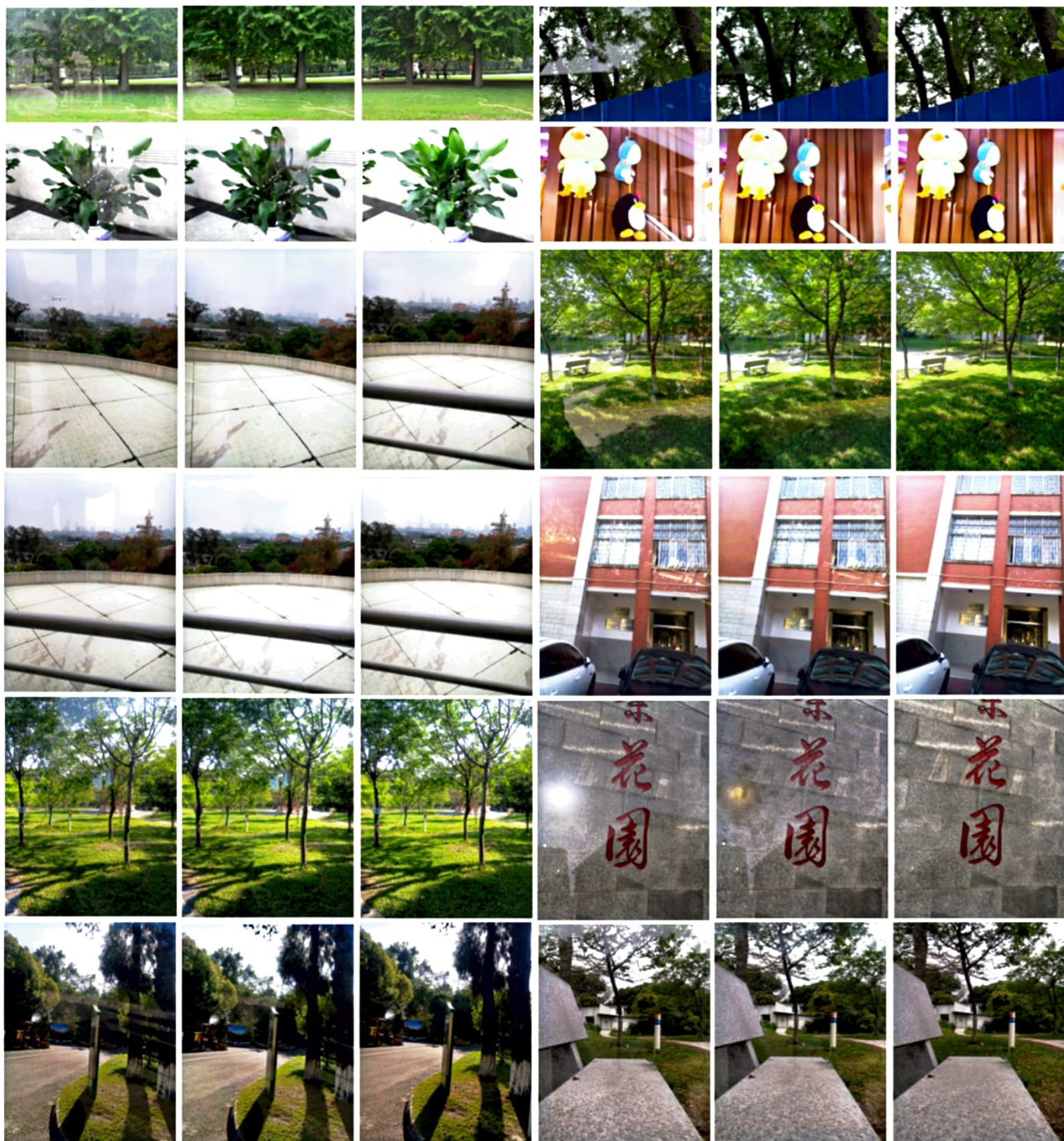


(e) T : Our ISP1



(f) T : Our ISP2

Figure 7. The first row shows that our ISP generates similar results compared with Lightroom and Camera Output. The second row shows that different ISPs can be applied to T to achieve similar results. Note that Lightroom is a professional ISP software supported by Adobe.



Input

RABRRN

Ground-truth

Input

RABRRN

Ground-truth

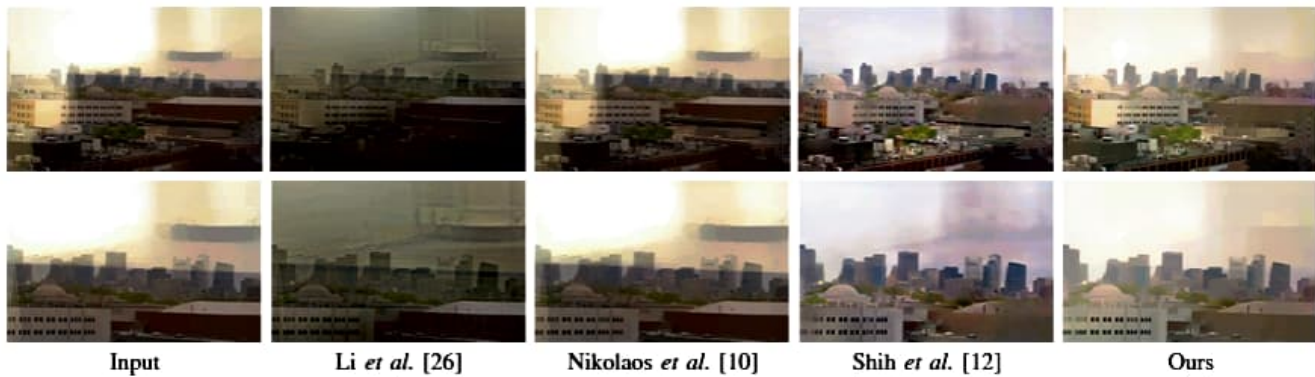


Fig. 12: Results on image "Factory".

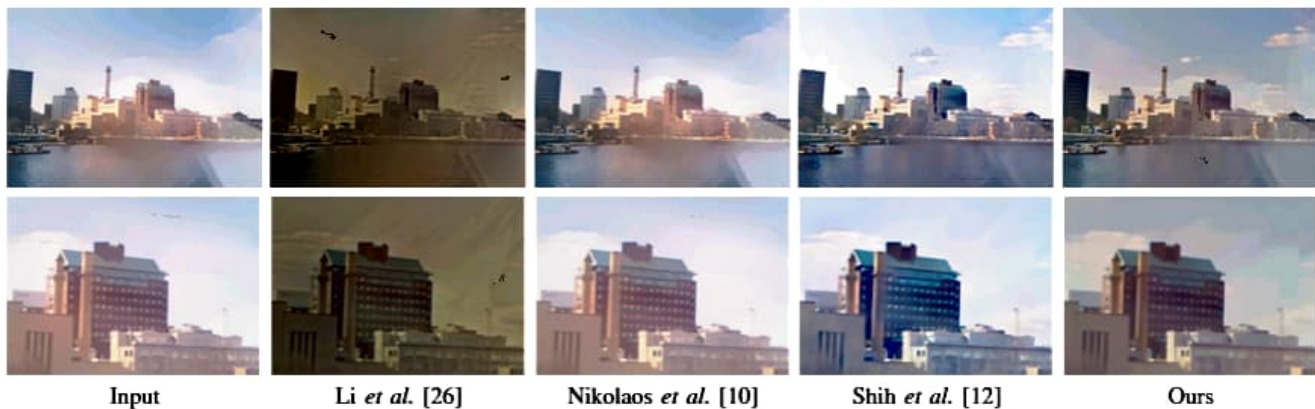


Fig. 13: Results on image "Lake".

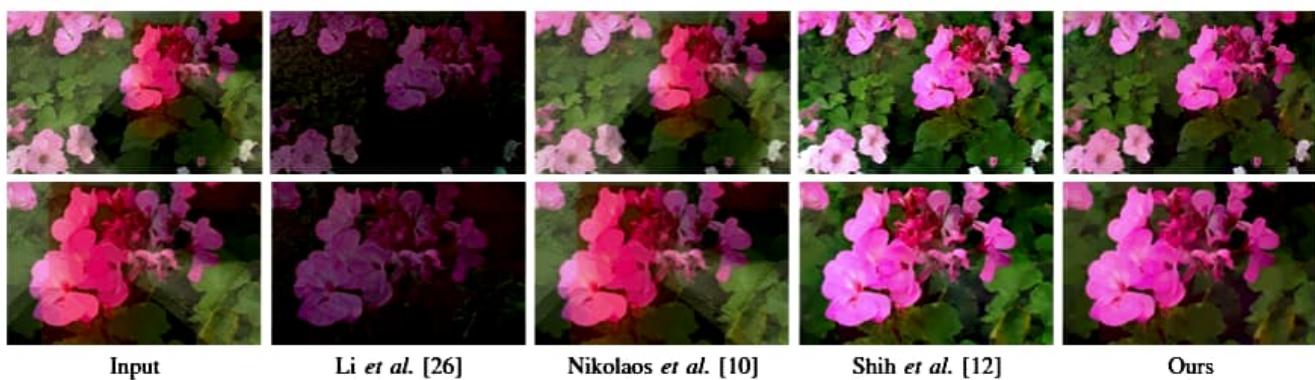


Fig. 14: Reflection results on image "Flower".

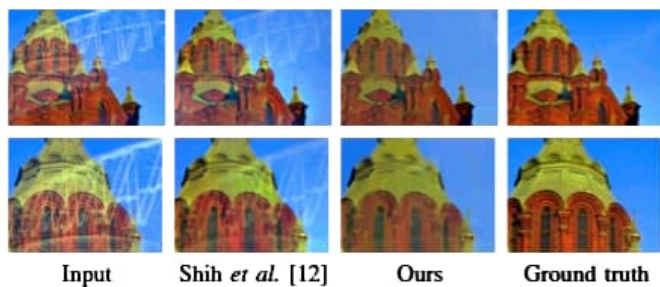


Fig. 15: Results on image "Church".

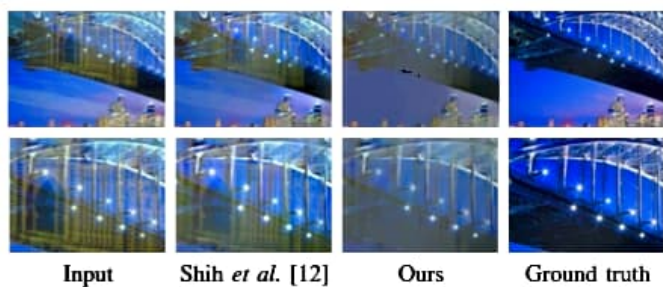


Fig. 16: Results on image "Bridge".



Input

BDN

ERRNet

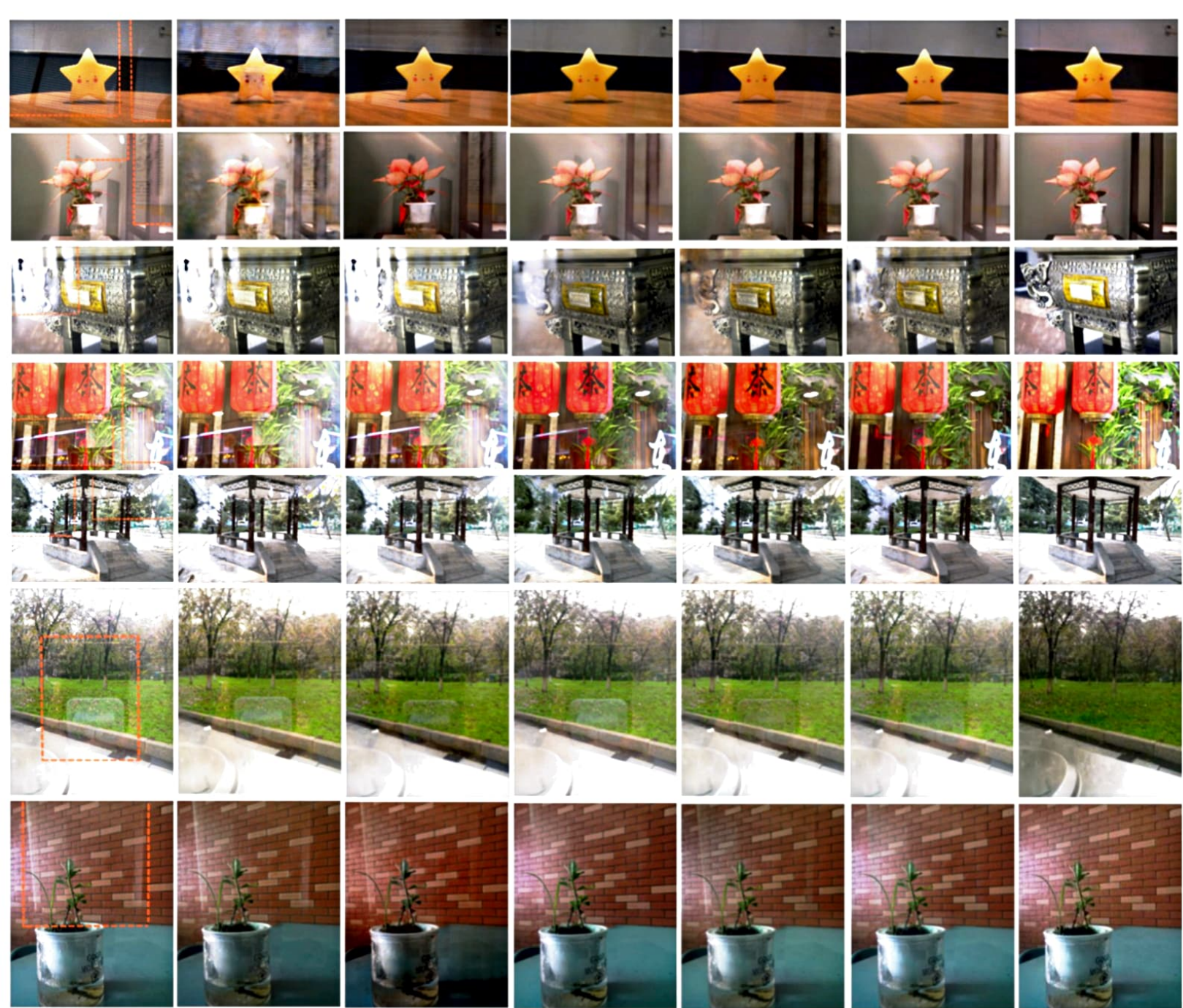
IBCLN

Kim *et al.*Chang *et al.*Peng *et al.*

Ours

GT







Ours-*M1*

Ours-*R1*

Ours-*M2*

Ours-*R2*

Figure 4. With the M-R pipeline proposed by Lei et al. [14], we can utilize a diverse set of glasses existing in our daily life (e.g., the curved and colored glass on the telephone booth, and the glass as a door).



Input

RAGNet_F

RAGNet_{FoM}

RAGNet_{FoM^{2c}}

RAGNet

Input

IBCLN

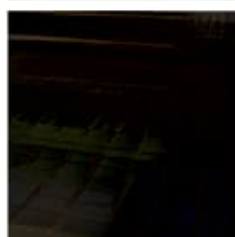
ERRNet

YTMT
UCS/UCT

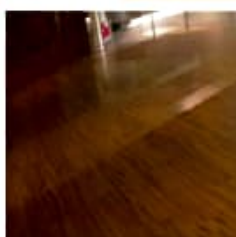
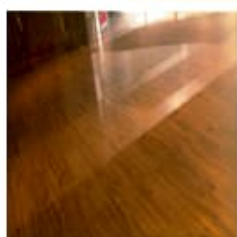
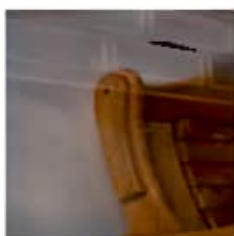
RPEN+PRRN

GT

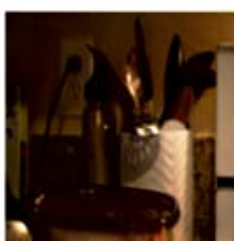
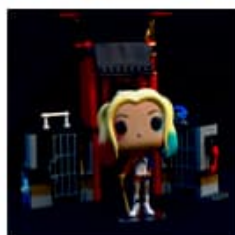
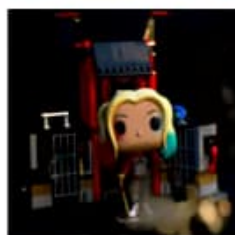
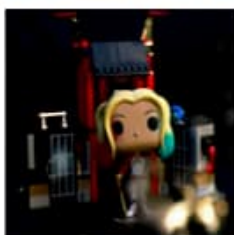
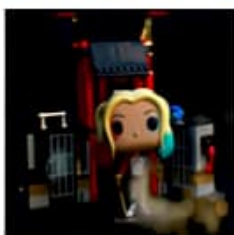
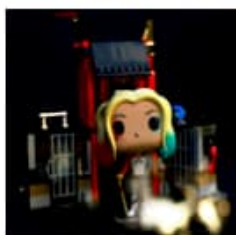
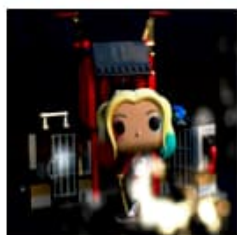
SRST



BRST



Real20





Input

RAGNet $_{I \rightarrow T}$

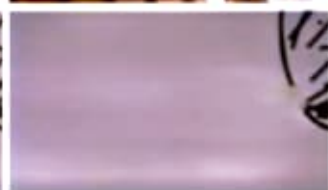
w/o \mathbf{F}_{diff}

w/o \mathcal{L}_{mask}

w/o $\mathcal{L}_{mask}^{diff}$

w/o \mathcal{L}_{mask}^{reg}

RAGNet



Input

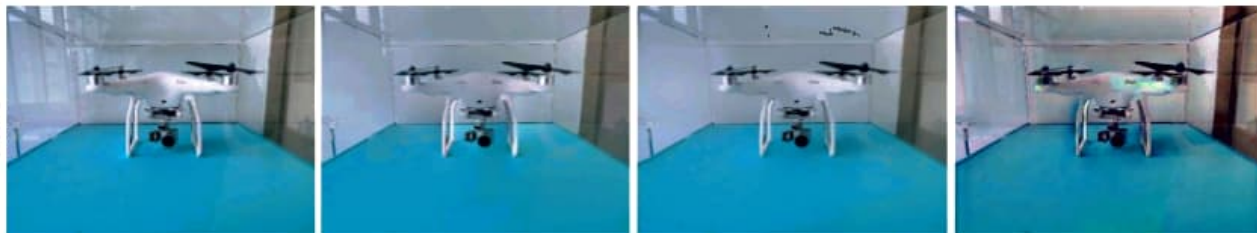
ERRNet

IBCLN

Predicted \hat{R}

Ours

BRST

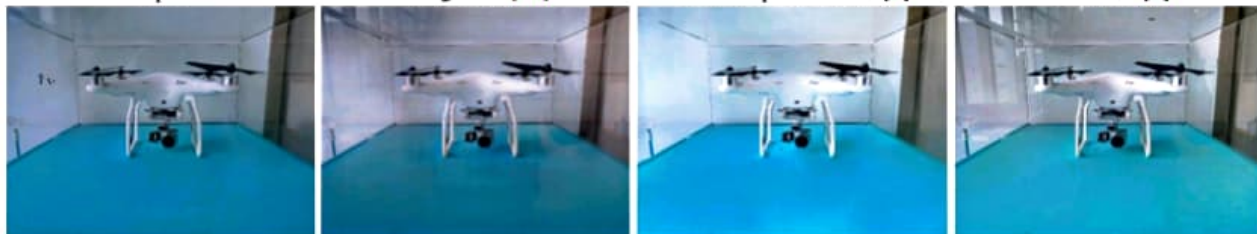


Input

Yang et al. [36]

Arvanitopoulos et al. [3]

CEILNet [5]



CoRRN [29]

Zhang et al. [38]

BDN [35]

Wei et al. [31]

SRST



Input

GT

Zhang et al. [38]

Wei et al. [31]



CoRRN [29]

BDN [35]

Yang et al. [36]

Li et al. [17]

Figure 8. Most methods cannot remove the sharp reflection. This is probably because learning-based methods are trained on synthetic data where R is blurry. Learning free methods often assume reflection is blurry. However, sharp reflection is quite common in the real world. Figure best viewed in the electronic version.

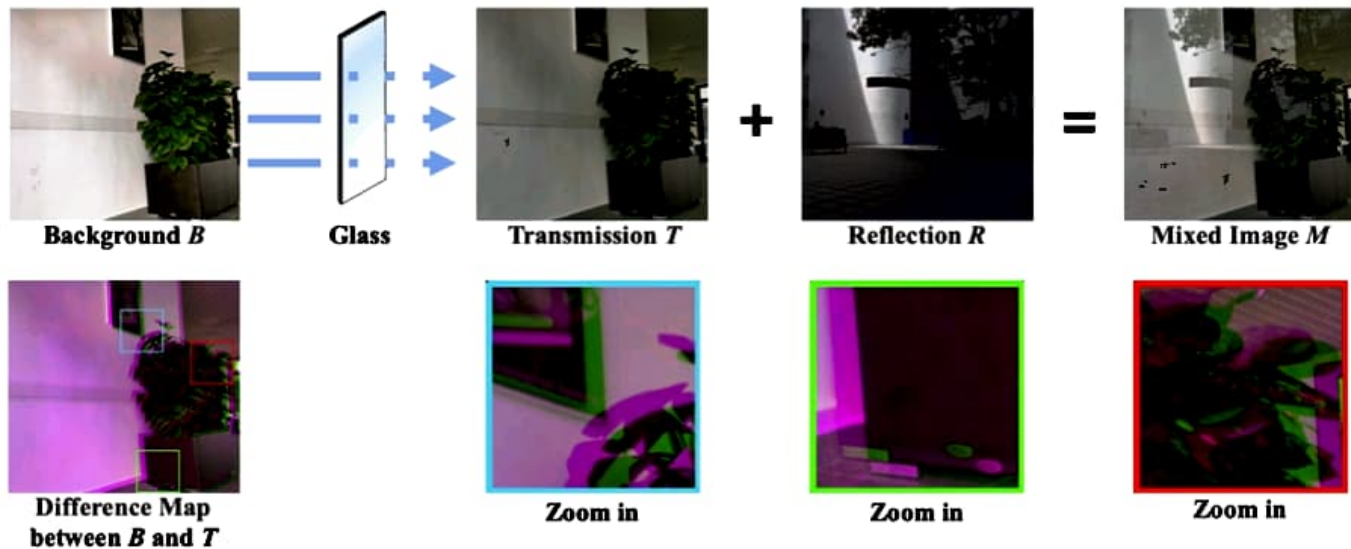
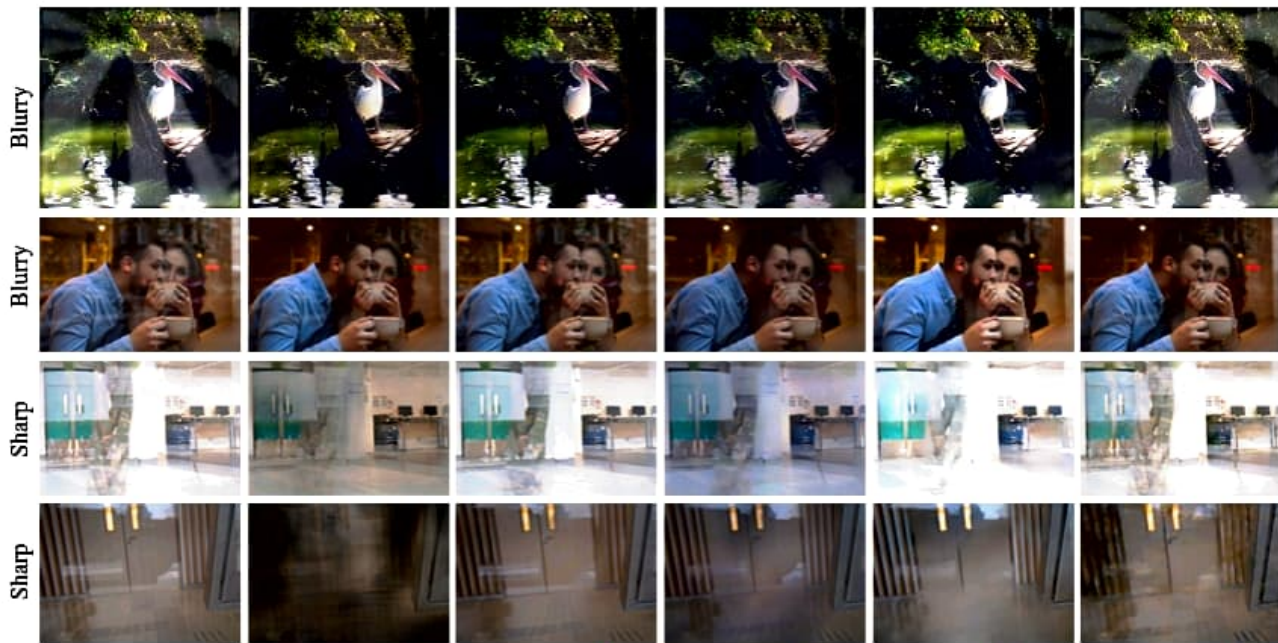


Figure 2. Due to refraction, spatial shift and intensity difference exist between B and T . The difference map visualizes the misalignment between B and T . The sum of the reflection R and the transmission T equals to the mixed image M in the raw data space.



Input

Zhang et al. [38]

Wei et al. [31]

CoRRN [29]

BDN [35]

Wen et al. [32]

Figure 1. The performance of existing methods on different types of reflection is quite different. Most algorithms can remove the blurry reflection but cannot remove the sharp reflection well.

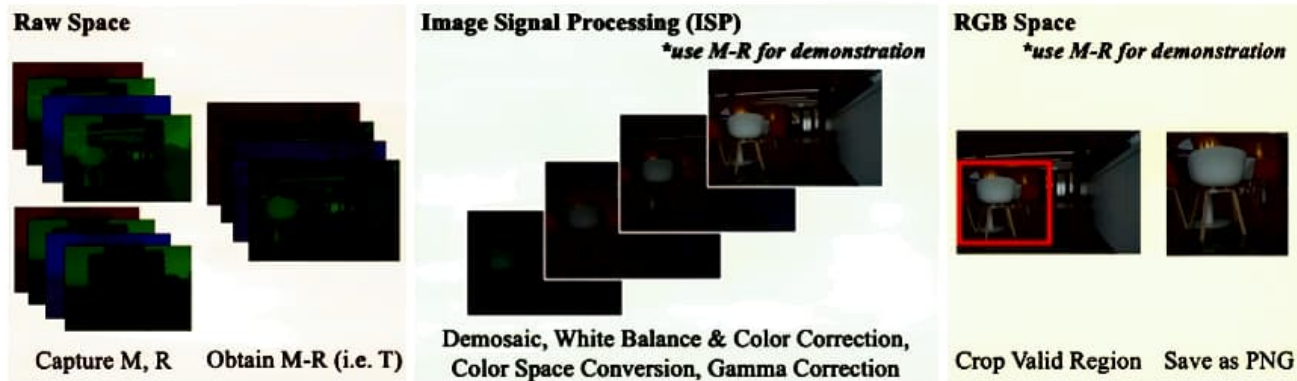


Figure 5. The post-processing pipeline. Ground-truth transmission T is obtained in the RAW space. Then all the RAW images are passed through an “ISP” to obtain the corresponding RGB images. Finally, the regions of interest regions are cropped out.



Observation I



Predicted Reflection \hat{R}



Visualization of $I - \hat{R}$



Ours



CEILNet [4]



BDN [9]



Lei et al. [13]



IBCLN [12]



Input

B:



R:



Proposed

CEILNet

PLNet

LS-SIFTF

SID

LS-DS



Input

B:



R:



Proposed

CEILNet

PLNet

LS-SIFTF

SID

LS-DS

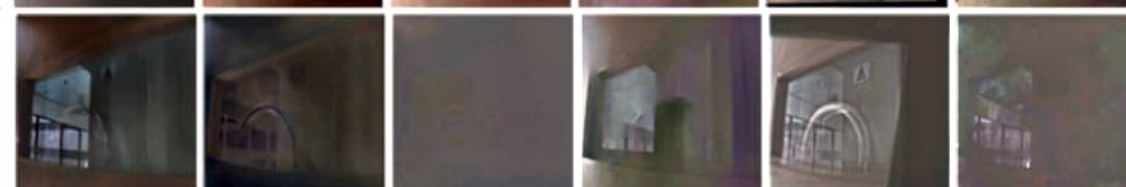


Input

B:



R:



Proposed

CEILNet

PLNet

LS-SIFTF

SID

LS-DS



Input

B:



R:



Proposed

CEILNet

PLNet

LS-SIFTF

SID

LS-DS



RGB M



RGB R



RGB $M - R$



Gamma $M - R$



Raw $M - R$

Figure 6. If $M - R$ is applied other than the raw data space, undesirable residuals will appear. "RGB $M - R$ ": do $M - R$ on RGB images. "Gamma $M - R$ ": use $M^{2.2} - R^{2.2}$ to reduce the impact of gamma correction. "Raw $M - R$ ": do $M - R$ on raw data.



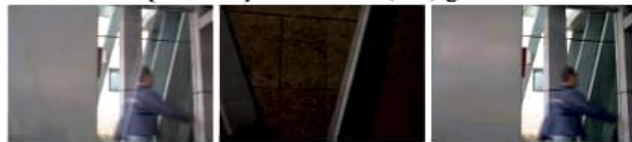
$\{M, R, T\}$ on curved glass



$\{M, R, T\}$ on colored (red) glass



$\{M, R, T\}$ on dynamic transmission



$\{M, R, T\}$ on dynamic transmission

Figure 3. More examples about the data diversity. In addition to glass types, we are also able to capture dynamic scenes, which enriches the scene diversity.



Input

Shih *et al.* [12]

Ours

Ground truth

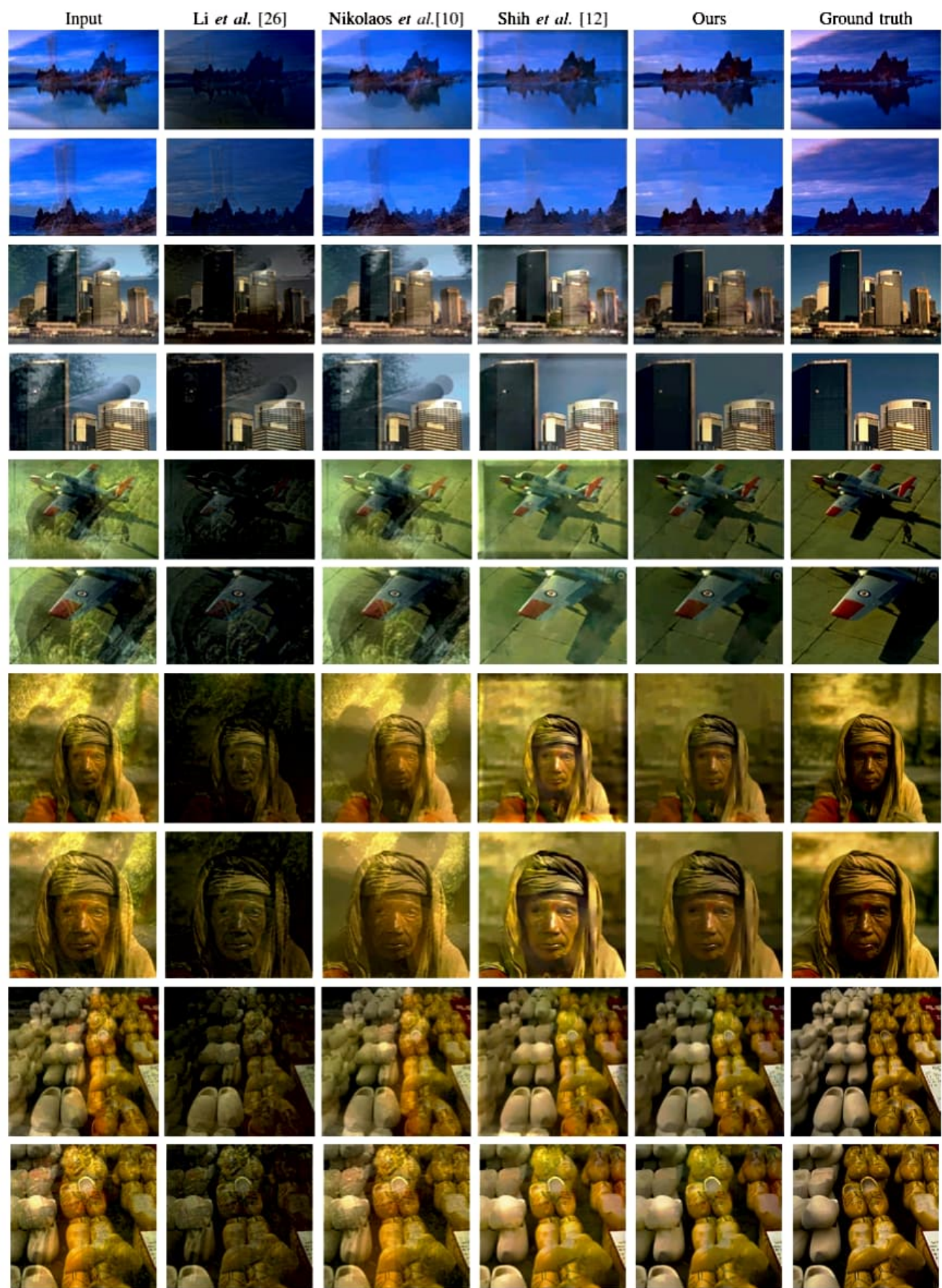


Fig. 11: The results on synthetic images. The odd/even rows show the whole/zoomed-in results.

